RECOMBINATION AND THE COSMIC MICROWAVE BACKGROUND

Once Big Bang Nucleosynthesis is over, at time $t \sim 300\,\mathrm{s}$ and temperature $T \sim 8 \times 10^8\,\mathrm{K}$, the Universe is a thermal bath of photons, protons, helium nuclei, traces of other light elements, and electrons, in addition to neutrinos and the unknown dark matter particle(s). The energy density is dominated by the relativistic component, photons and neutrinos. With the exception of neutrinos and the dark matter which by this time have decoupled from the plasma, all particle species have the same temperature which is established by interactions of charged particles with the photons.

Photons interacted primarily with electrons through Thomson scattering:

$$\gamma + \mathrm{e}^- \rightarrow \gamma + \mathrm{e}^-$$

i.e. the elastic scattering of electromagnetic radiation by a free charged particle. Thomson scattering is the low-energy limit of Compton scattering and is a valid description in the regime where the photon energy is much less than the rest-mass energy of the electron. In this process, the electron can be thought of as being made to oscillate in the electromagnetic field of the photon causing it, in turn, to emit radiation at the same frequency as the incident wave, and thus the wave is scattered. An important feature of Thomson scattering is that it introduces polarization along the direction of motion of the electron (see Figure 9.1). The cross-section for Thomson scattering is tiny:

$$\sigma_\mathrm{T} = \frac{1}{6\pi\epsilon_0^2}\left(\frac{\mathrm{e}^2}{m_\mathrm{e}c^2}\right)^2 = 6.6 \times 10^{-25}\,\mathrm{cm}^2 \qquad (9.1)$$

and therefore Thomson scattering is most important when the density of free electrons is high, as in the early Universe or in the dense interiors of stars.[1]

[1]Photons are also scattered by free protons, but σ_T for proton scattering is smaller by a factor $(m_\mathrm{e}/m_\mathrm{p})^2$ (eq. 9.1), so it can be neglected. It is the Coulomb interaction with the electrons that keeps the protons in thermal equilibrium with the electrons and photons.

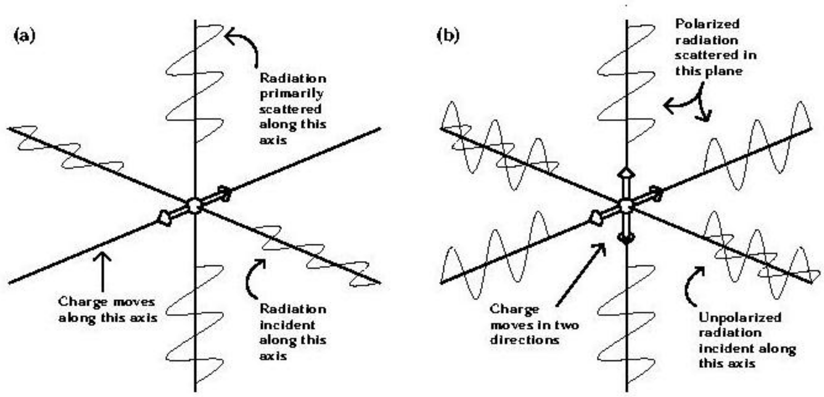

Figure 9.1: Schematic diagram of Thomson scattering with the electron being illuminated from a single direction. The two cases correspond to the incident light being either (a) linearly polarized or (b) unpolarized. For clarity, only the electric field of the radiation propagating along the coordinate axes is illustrated.

The scattering rate per photon, $\Gamma_{\rm T,e}$, can be estimated as follows. The mean free path for photons (the mean distance travelled between scatterings) is

$$\lambda = \frac{1}{n_{\rm e}\sigma_{\rm T}} \tag{9.2}$$

where $n_{\rm e}$ is the electron density, and the rate at which a photon undergoes scattering is therefore:

$$\Gamma_{\rm T,e} = \frac{c}{\lambda} = n_{\rm e}\sigma_{\rm T}c\,. \tag{9.3}$$

The *optical depth* to Thomson scattering is the integral over time of the scattering rate:

$$\tau = \int \Gamma_{\rm T,e}(t)\,dt\,. \tag{9.4}$$

When the Universe is fully ionised, $n_{\rm e} \simeq n_{\rm b} = n_{\rm b,0}\,(1+z)^3$ (neglecting the neutrons bound within atomic nuclei), from which we deduce:

$$\begin{aligned}\Gamma_{\rm T,e} &\simeq 2.5\times10^{-7}\cdot 6.6\times10^{-25}\cdot 3\times10^{10}\,(1+z)^3\,{\rm s}^{-1}\\ &\simeq 5\times10^{-21}\,(1+z)^3\,{\rm s}^{-1}\end{aligned} \tag{9.5}$$

where we have used $n_{\rm b,0} = 2.5\times10^{-7}\,{\rm cm}^{-3}$ from eq. 7.5.

9.1 Matter Domination

The next important milestone in the Universe history is the transition from a radiation-dominated to a matter-dominated regime. Recalling the full expression for $H(z)$:

$$\frac{H(z)}{H_0} = \sqrt{\Omega_{\mathrm{m},0}(1+z)^3 + \Omega_{\mathrm{rad},0}(1+z)^4 + \Omega_{\mathrm{k},0}(1+z)^2 + \Omega_{\Lambda,0}}\,, \tag{9.6}$$

it can be seen immediately that

$$z_{\mathrm{eq}} = \frac{\Omega_{\mathrm{m},0}}{\Omega_{\mathrm{rad},0}} - 1 \simeq 3380 \tag{9.7}$$

(with $\Omega_{\mathrm{rad},0} \simeq 9 \times 10^{-5}$ which includes the contribution from neutrinos), when the temperature was $T_{\mathrm{eq}} = 2.7255 \times 3381 = 9215\,\mathrm{K}$. After this epoch, the expansion rate is driven by pressureless matter (i.e what we called *dust* in Lecture 1), until either the curvature or, if $\Omega_{\mathrm{k},0} = 0$, the Λ term starts to dominate.

9.2 Recombination

As the Universe cools further, a time comes when it is thermodynamically favourable for ions (protons and He^{2+} nuclei) and electrons to combine and form neutral atoms. This is the epoch of recombination, the next important transition in the history of our Universe. With the rapidly diminishing density of free electrons, the photon scattering rate, $\Gamma_{\mathrm{T,e}}$, drops below the expansion rate H, the photons decouple from the electrons and can stream freely (their mean free path becomes very much longer): the Universe is now transparent to radiation. Thus, as we look back in time with even our most powerful photon-collecting telescopes, the epoch of recombination is the ultimate frontier, the furthest location and the earliest time we can reach with electromagnetic radiation. Once photon and baryons have decoupled, the latter are no longer compelled to have the the same temperature as the photons.

The temperature at which recombination takes place depends on the baryon-to-photon ratio, η, and on the ionisation potential of the species involved. For simplicity, we shall limit ourselves to H with ionisation potential $Q = 13.6\,\mathrm{eV}$ from the ground state, and ignore He with ionisation potentials of $24.6\,\mathrm{eV}$ and $54.4\,\mathrm{eV}$ to form He^+ and He^{2+} respectively.

Before recombination, the reaction in question:

$$\mathrm{H} + \gamma \rightleftharpoons \mathrm{p} + \mathrm{e}^-$$

is in statistical equilibrium, with the photoionization rate balancing the radiative recombination rate. In statistical equilibrium at temperature T, the number density n_x of particles with mass m_x is given by the Maxwell-Boltzmann equation:

$$n_\mathrm{x} = g_\mathrm{x} \left(\frac{m_\mathrm{x}\, kT}{2\pi\hbar^2} \right)^{3/2} \exp\left[-\frac{m_\mathrm{x} c^2}{kT} \right] , \tag{9.8}$$

where g_x is the statistical weight of particle x. This expression applies in the non-relativistic regime, i.e. when $kT \ll m_\mathrm{x} c^2$.

Writing eq. 9.8 for H atoms, protons and free electrons, we can construct an equation that relates the number densities of these particles:

$$\frac{n_\mathrm{H}}{n_\mathrm{p} n_\mathrm{e}} = \frac{g_\mathrm{H}}{g_\mathrm{p} g_\mathrm{e}} \left(\frac{m_\mathrm{H}}{m_\mathrm{p} m_\mathrm{e}} \right)^{3/2} \left(\frac{kT}{2\pi\hbar^2} \right)^{-3/2} \exp\left[\frac{(m_\mathrm{p} + m_\mathrm{e} - m_\mathrm{H}) c^2}{kT} \right] \tag{9.9}$$

Eq. 9.9 can be simplified further considering that: (i) the ratio of the statistical weights is 1; (ii) $m_\mathrm{H} \simeq m_\mathrm{p}$; and (iii) the term in the numerator of the exponential factor is the binding energy of the H atom, i.e. the ionisation potential Q. With these simplifications, we obtain the Saha equation:

$$\frac{n_\mathrm{H}}{n_\mathrm{p} n_\mathrm{e}} = \left(\frac{m_\mathrm{e}\, kT}{2\pi\hbar^2} \right)^{-3/2} \exp\left[\frac{Q}{kT} \right] . \tag{9.10}$$

What we want to do now is to use the Saha equation to deduce the ionisation fraction:

$$X \equiv \frac{n_\mathrm{p}}{n_\mathrm{p} + n_\mathrm{H}} = \frac{n_\mathrm{p}}{n_\mathrm{b}} = \frac{n_\mathrm{e}}{n_\mathrm{b}} \tag{9.11}$$

as a function of T and η. With the above definition (which implicitly assumes charge neutrality in the Universe), $X = 1$ when the baryons are fully ionised, $X = 0.5$ when half of the baryons are ionised, and $X = 0$ when the baryons are all in neutral atoms.

With the substitutions:

$$n_\mathrm{H} = \frac{1-X}{X} n_\mathrm{p}, \qquad n_\mathrm{e} = n_\mathrm{p} ,$$

we can re-write eq. 9.10 as:

$$\frac{1-X}{X} = n_\mathrm{p} \left(\frac{m_\mathrm{e}\, kT}{2\pi\hbar^2} \right)^{-3/2} \exp\left[\frac{Q}{kT} \right] \tag{9.12}$$

We can express n_p in terms of η:

$$\eta = \frac{n_\mathrm{p}}{X n_\gamma}$$

where for a blackbody spectrum:

$$n_\gamma = \frac{2.404}{\pi^2}\left(\frac{kT}{\hbar c}\right)^3 = 0.244\left(\frac{kT}{\hbar c}\right)^3$$

so that:

$$n_\mathrm{p} = 0.244 X\eta\left(\frac{kT}{\hbar c}\right)^3$$

which we can now substitute into eq. 9.12 to give

$$\frac{1-X}{X^2} = 3.84\eta\left(\frac{kT}{m_\mathrm{e}c^2}\right)^{3/2}\exp\left[\frac{Q}{kT}\right]. \tag{9.13}$$

Solving the quadratic equation in X, we find that the positive root is

$$X = \frac{-1+\sqrt{1+4S}}{2S} \tag{9.14}$$

where

$$S(T,\eta) = 3.84\eta\left(\frac{kT}{m_\mathrm{e}c^2}\right)^{3/2}\exp\left[\frac{Q}{kT}\right]. \tag{9.15}$$

Note that when $kT \gg Q$, $X \simeq 1$ and the gas is close to being fully ionised. Once kT falls below Q, $X \to 0$; however, both η and the term $(kT/m_\mathrm{e}c^2)^{3/2}$ are small numbers, and their product is overcome by the exponential term only once the temperature has fallen well below the binding energy.

We can solve eq. 9.15 numerically to find the value of T when $X = 0.5$ which we define to be the epoch of recombination (half of the baryons ionised and half of them neutral). With $\eta = 6.1 \times 10^{-10}$, we have:

$$kT_\mathrm{rec} = 0.323\,\mathrm{eV} = \frac{Q}{42}. \tag{9.16}$$

Scaling back $T_\mathrm{CMB,0} = 2.7255\,\mathrm{K}$ to $T_\mathrm{rec} = 0.323\,\mathrm{eV} \equiv 3750\,\mathrm{K}$, we find $(1+z_\mathrm{rec}) = 1375$, which corresponds to time $t_\mathrm{rec} = 251\,000\,\mathrm{yr}$.

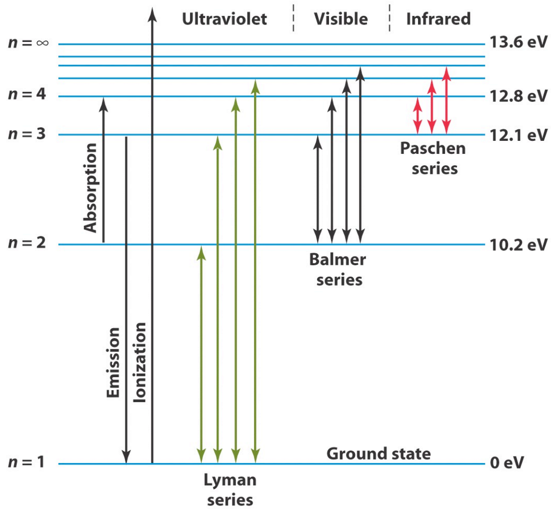

Figure 9.2: Energy levels of the H atom.

9.3 Photon Decoupling

Recombination was not an instantaneous process but proceeded relatively quickly nevertheless, with the fractional ionisation decreasing from $X = 0.9$ to $X = 0.1$ over a time interval $\Delta t \sim 70\,000\,\mathrm{yr}$. With the number density of free electrons dropping rapidly, the time when photons and baryons decoupled follows soon, once the rate for Thomson scattering $\Gamma_{\mathrm{T,e}}$ falls below the expansion rate H.

The exact calculation of z_{dec} is complicated by the fact that the Saha equation used to derive $X(T)$ assumes that the reaction $\mathrm{H} + \gamma \rightleftharpoons \mathrm{p} + \mathrm{e}^-$ is in equilibrium, but this is no longer the case when $\Gamma_{\mathrm{T,e}}$ drops below H. In reality, the photon-baryon fluid remains *overionised* for its temperature compared to the equilibrium condition under which the Saha equation applies (see Figure 9.3), as can be appreciated by considering the following.

If the recombination $\mathrm{p} + \mathrm{e}^- \rightarrow \mathrm{H} + \gamma$ takes place directly to the ground state ($n = 1$) of hydrogen, the emitted photon with $E = h\nu = 13.6\,\mathrm{eV}$ can readily ionise a H atom, with no net effect (see Figure 9.2). Radiative recombination to a higher energy level with subsequent decay to the ground state does not help either towards a lower ionisation fraction, for similar reasons: the emitted photons will quickly be reabsorbed by H atoms, which are then promptly reionised given the high density of photons with $E < 13.6\,\mathrm{eV}$.[2]

[2]This is a common problem in astrophysics, whereby Lyman α photons are *resonantly scattered*. In ionised regions around hot stars (H II regions), such photons eventually either escape the nebula at different frequencies from the resonant frequency (after many resonant scatterings), or are converted into infrared photons by heating interstellar dust grains.

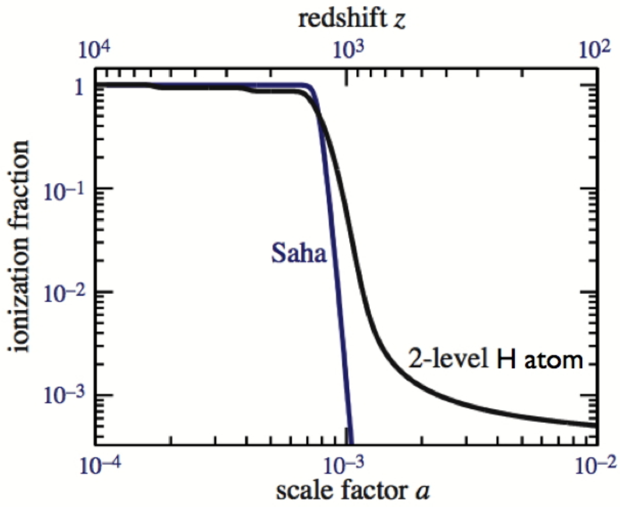

Figure 9.3: A full treatment that includes the energy levels of the H atom and the trapping of Lyman photons within the plasma shows that the baryons remain overionised relative to the equilibrium conditions implicit in the Saha equation. As a result, photon-baryon decoupling is delayed and more protracted.

Ultimately, the process that drives X to lower values is *two-photon emission* from the 2S to the 1S ground state. This transition is highly forbidden, with a transition probability $\sim 10^8$ lower than the Lyman α line from 2P to 1S. In order to conserve energy and angular momentum, a pair of photons is emitted, neither of which is energetic enough to excite an atom from the ground state. This breaks the bottleneck and provides a net sink of energetic photons. Taking into account all the relevant processes, it is found that $z_{\rm dec} = 1090$, when $T_{\rm dec} = 2971$ K and $t_{\rm dec} = 372\,000$ yr.

After their last scattering off an electron, photons were able to travel unimpeded through the Universe.[3] These are the Cosmic Microwave Background photons we receive today, still with their blackbody distribution, now redshifted by a factor of 1091. They constitute a *last scattering surface*, or more appropriately a *last scattering layer*, since (obviously) not all photons underwent their last scattering simultaneously: just as we can see in little distance into a fog bank on Earth, we can penetrate a little way into the 'electron fog' that hides earlier times from our direct view (see Figure 9.4).

Of course, there is nothing special about this particular surface, other than it happens to be at the right distance for the photons to have reached us

[3]With the exception of photons with energies greater than 10.2 eV (with wavelengths $\lambda \leq 1215.67$ Å) which are absorbed efficiently by neutral hydrogen. However, such photons are comparatively small in number, being far out in the Wien tail of the blackbody distribution for $T_{\rm dec} = 2971\,{\rm K} = 0.256$ eV.

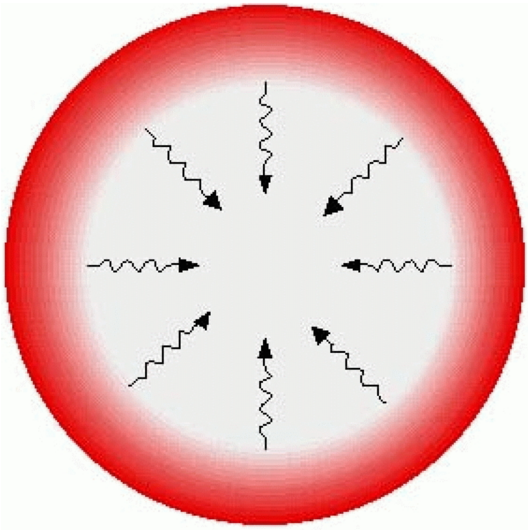

Figure 9.4: The last scattering layer.

today. There are photons originating at every point, and observers in different parts of the Universe will see photons originating from different large spheres, of the same radius, centred on their location.

What is important is that the existence of an isotropic photon background with a blackbody spectrum is a natural consequence of an earlier, denser and hotter phase in the Universe history, when photons and baryons existed in a highly interacting thermal state. The existence of this radiation is one of the pillars on which the model of a hot Big Bang rests. Any other interpretation of the CMB has to invoke rather contrived scenarios.

The table below summarises the cosmic epochs discussed in this lecture.

Table 9.1 Cosmic epochs considered in this lecture

Event	Redshift	T (K)	t (Myr)
Radiation-Matter Equality	3380	9215	0.047
Recombination	1375	3750	0.251
Photon Decoupling	1090	2971	0.372
Last Scattering	1090	2971	0.372

9.4 The Cosmic Microwave Background

The Cosmic Microwave Background radiation was discovered serendipitously in 1965 by two American radio astronomers, Arno Penzias and Robert Wilson, while trying to identify sources of noise in microwave satellite communications at Bell Laboratories in New Jersey.[4] Their discovery was announced alongside the interpretation of the CMB as relic thermal radiation from the Big Bang by Robert Dicke and collaborators working at the nearby Princeton University. Interestingly, the possibility of a cosmic thermal background were first entertained by Gamow, Alpher and Herman in 1948 as a consequence of Big Bang nucleosynthesis, but the idea was so beyond the experimental capabilities of the time that it fell into obscurity in the intervening two decades.

The average energy of a CMB photon today, $\langle h\nu \rangle = 6.3 \times 10^{-4}\,\mathrm{eV}$, is tiny compared to the energies required to break up atomic nuclei ($\sim 1\,\mathrm{MeV}$), or excite atomic energy levels ($\sim 10\,\mathrm{eV}$), but comparable to the energy differences between vibrational and rotational levels of some molecules, including H_2O. Thus, after their 13.8 Gyr journey through the cosmos, from the surface of last scattering to us, CMB photons are absorbed a microsecond away from the Earth's surface by a water molecule in the atmosphere of our planet. The original detection by Penzias and Wilson was at a wavelength of 73.5 mm, this being the wavelength of the telecommunication signals they were working with; this wavelength is two orders of magnitude longer than $\lambda_{\mathrm{peak}} = 1.1\,\mathrm{mm}$ of a $T = 2.7255\,\mathrm{K}$ blackbody.

For this reason, observations of the CMB over the last 50 years have been conducted primarily from satellites, but also from high altitude balloons and from Antarctica, where the water content of the atmosphere is very low. The successive space missions COBE, WMAP and Planck have built an increasingly accurate map of the CMB radiation over the entire sky. Encoded in this map is a comprehensive description of the cosmological parameters that define our Universe—a topic that we will explore in detail in the next lecture. It is a fitting measure of the importance of the CMB, that not only its discoverers (Penzias and Wilson), but also the principal

[4] Researchers working at Bell Labs are credited with the development of radio astronomy, the transistor, the laser, the charge-coupled device (CCD), information theory, the UNIX operating system, the C programming language, S programming language and the C++ programming language. Eight Nobel Prizes have been awarded for work completed at Bell Laboratories (from Wikipedia).

investigators of the COBE and WMAP missions have been awarded some of the most prestigious prizes in Physics and Astronomy.

Incidentally, the CMB provides the solution to Olbers' paradox: The sky at night (or during the day for that matter!) is indeed bright everywhere, but at the mm wavelengths of CMB photons, rather than the optical wavelengths of starlight.

Table 9.2 summarises the most important properties of the CMB.

Table 9.2 CMB parameters

Property	Value
Temperature, $T_{\rm CMB}$	$2.7255\,$K
Peak Wavelength, $\lambda_{\rm peak}$	$0.106\,$cm
Number density of CMB photons, $n_{\gamma,0}$	$411\,\mathrm{cm}^{-3}$
Energy density of CMB photons, $u_{\gamma,0}$	$0.26\,\mathrm{eV\ cm}^{-3}$
Average photon energy, $\langle h\nu_{\rm CMB}\rangle$	$6.34 \times 10^{-4}\,$eV
Photon/Baryon ratio, $1/\eta$	1.64×10^{9}

9.4.1 Isotropy of the CMB

At any angular position (θ, ϕ) on the sky, the spectrum of the CMB is a near-perfect blackbody (see Figure 9.5). The CMB is in fact the closest approximation we have to an ideal blackbody, much closer than, for example, the spectral distribution of stars, and closer than any blackbody

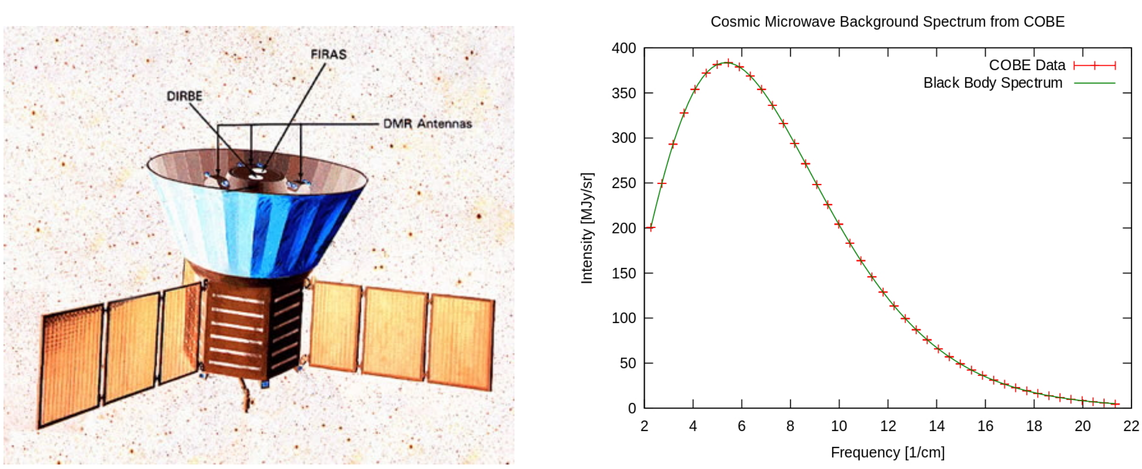

Figure 9.5: The spectral shape of the Cosmic Microwave Background measured by the COBE satellite is that of a blackbody with temperature $T = 2.7255\,$K.

emitter we have been able to build in a laboratory on Earth.

With $T(\theta, \phi)$ denoting the temperature at a given point on the sky, the mean temperature averaged over the whole sky is:

$$\langle T \rangle = \frac{1}{4\pi} \int T(\theta, \phi) \sin\theta \, d\theta \, d\phi = 2.7255 \pm 0.0006 \, \mathrm{K} \, . \tag{9.17}$$

The deviations from this mean temperature from point to point on the sky are tiny. Defining the dimensionless T fluctuations:

$$\frac{\delta T}{T}(\theta, \phi) = \frac{T(\theta, \phi) - \langle T \rangle}{\langle T \rangle} \, , \tag{9.18}$$

it is found that:

$$\left\langle \left(\frac{\delta T}{T} \right)^2 \right\rangle^{1/2} = 1.1 \times 10^{-5} \, . \tag{9.19}$$

Such deviations were first reported in 1992 by the COBE team. Subsequent CMB missions (WMAP and Planck) have significantly improved the angular resolution and precision in the mapping of the CMB sky, as illustrated in Figure 9.6.

The finding that the temperature of the CMB varies by only 30 μK across the whole sky is strong evidence for an isotropic (and therefore presumably homogeneous) Universe. However, it also presents us with a significant

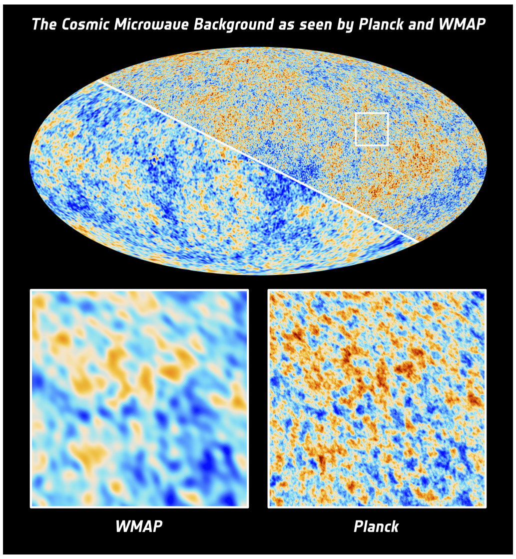

Figure 9.6: Tiny anisotropies (at the level of $\delta T/T \sim 10^{-5}$) in the temperature of the Cosmic Microwave Background, as recorded by the WMAP and Planck satellites.

puzzle: how can we explain such a high degree of isotropy? To understand what motivates this question, consider the following.

Naively, one may expect the size of the region over which isotropy pertains to be the horizon scale at the time of photon decoupling. Regions further apart than the light-travel distance at $z_{\rm dec}$ wouldn't know about each other, that is they are not causally connected. Put in a different way, heat transfer could equalise the temperature between regions slightly hotter and slightly colder than the mean only up to a maximum distance, given by $ct_{\rm dec}$.

Recalling our discussion of horizons in section 5.3.2, we can re-write eq. 5.24 as the *comoving* horizon distance at time t:

$$s_{\rm hor,com}(t) = \int_0^t \frac{c\,{\rm d}t}{a(t)} \; . \qquad (9.20)$$

We want $s_{\rm hor}$ at redshift z. Using $\dot{a} = {\rm d}a/{\rm d}t$, ${\rm d}t = {\rm d}a/\dot{a} = {\rm d}a/aH$, we have:

$$s_{\rm hor,com}(a) = \int_0^a \frac{c\,{\rm d}a}{a^2 H(a)} \; . \qquad (9.21)$$

Our usual expression for the Hubble parameter as a function of $a \equiv (1+z)^{-1}$:

$$\frac{H(a)}{H_0} = \left(\Omega_{\rm rad,0}\, a^{-4} + \Omega_{\rm m,0}\, a^{-3} + \Omega_{\rm k,0}\, a^{-2} + \Omega_{\Lambda,0}\right)^{1/2} \qquad (9.22)$$

reduces to:

$$H(a) \simeq H_0 \sqrt{\Omega_{\rm m,0}}\, a^{-3/2} \qquad (9.23)$$

at $z_{\rm dec} = 1090$, when the expansion has been dominated by the energy density of matter for most of the age of the Universe (see Table 9.1). With (9.23), we can re-write (9.21) as:

$$s_{\rm hor,com}(a) \simeq \frac{c}{H_0}\, \Omega_{\rm m,0}^{-1/2} \int_0^a \frac{1}{a^{1/2}} {\rm d}a \; . \qquad (9.24)$$

Performing the simple integration and now changing to redshift, we have:

$$s_{\rm hor,com}(z) \simeq 2 \frac{c}{H_0}\, \Omega_{\rm m,0}^{-1/2} (1+z)^{-1/2} \, , \qquad (9.25)$$

or

$$s_{\rm hor,prop}(z_{\rm dec}) \simeq 2\frac{c}{H_0}\,\Omega_{\rm m,0}^{-1/2}(1+z_{\rm dec})^{-3/2}\,. \tag{9.26}$$

where $s_{\rm hor,prop} = a\,s_{\rm hor,com}$ is the physical (proper) horizon distance at decoupling.

The angle on the sky subtended by a length $s_{\rm hor,prop}$ is:

$$\theta_{\rm hor,dec} = \frac{s_{\rm hor,prop}(z_{\rm dec})}{d_{\rm A}(z_{\rm dec})} \tag{9.27}$$

where $d_{\rm A}$ is the angular diameter distance. In Lecture 5.3.3 we saw that in a flat universe ($\Omega_{\rm k,0} = 0$) the expression for d_A is simplified to:

$$d_{\rm A}(z) = \frac{c}{H_0}\,\frac{1}{(1+z)}\int\limits_0^z \frac{dz}{\left[\Omega_{\rm m,0}\,(1+z)^3 + \Omega_{\Lambda,0}\right]^{1/2}} \tag{9.28}$$

The elliptical integral is not of straightforward solution. However, in an open universe with $\Omega_{\Lambda,0} = 0$, $\Omega_{\rm k,0} \neq 0$, the so-called Mattig relation applies:

$$d_{\rm A}(z) = 2\frac{c}{H_0}\,\frac{1}{\Omega_{\rm m,0}^2\,(1+z)^2} \times \left[\Omega_{\rm m,0}z + (\Omega_{\rm m,0}-2)\,\left(\sqrt{1+\Omega_{\rm m,0}z}-1\right)\right] \tag{9.29}$$

which, for $z \gg 1$ reduces to:

$$d_{\rm A}(z) \approx 2\frac{c}{H_0}\,\frac{1}{\Omega_{\rm m,0}\,z}\,. \tag{9.30}$$

Substituting 9.30 and 9.26 into 9.27 we find:

$$\theta_{\rm hor,dec} \approx \left(\frac{\Omega_{\rm m,0}}{z_{\rm dec}}\right)^{1/2} = \left(\frac{0.312}{1090}\right)^{1/2} = 0.017\,\text{radians} \sim 1^\circ \tag{9.31}$$

In models with a cosmological constant ($\Omega_{\rm m,0} + \Omega_{\Lambda,0} = 1$, $\Omega_{\rm k,0} = 0$)

$$\theta_{\rm hor,dec} \approx 1.8^\circ$$

with a very weak dependence on $\Omega_{\rm m,0}$ ($\propto \Omega_{\rm m,0}^{-0.1}$).

What this means is that CMB photons coming to us from two directions separated by more than $\sim 2^\circ$ originated from regions which were not in causal contact at $z_{\rm dec}$. The fact that the CMB is uniform over much larger angular scales constitutes what is referred to as the **horizon problem**.

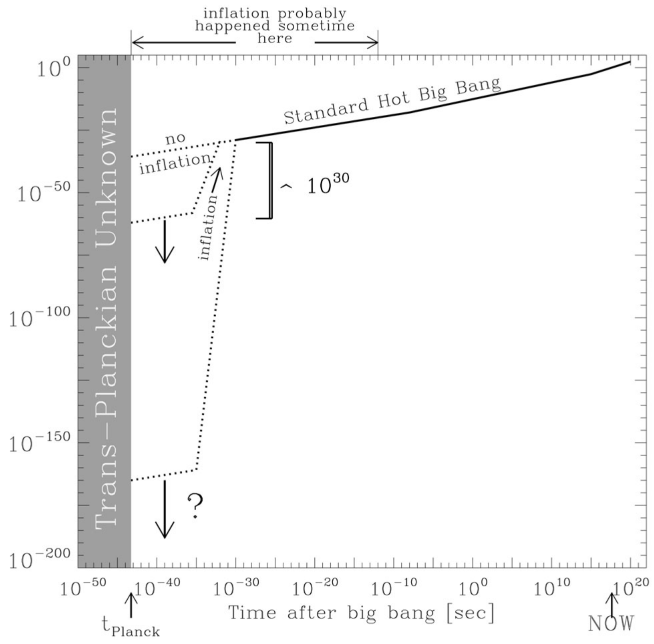

Figure 9.7: During an inflationary phase, the Universe expands exponentially. In this scenario, the whole Universe visible today was in causal contact prior to inflation, explaining the near-perfect isotropy of the CMB radiation (as well as other cosmological puzzles). (Figure credit: Charles Lineweaver).

A 'solution' to the horizon problem was formulated in 1980s. The horizon problem (and other cosmological puzzles) could be resolved if the entire Universe within our horizon had in fact been in causal contact at very early times, and had been inflated by a huge factor ($> 10^{30}$) during a brief period of exponential expansion (see Figure 9.7). This is the inflationary scenario, originally proposed by Alan Guth and now considered seriously by most cosmologists, being supported by several lines of evidence.

Inflation is suspected to be an event associated with the GUT transition at $t \sim 10^{-35}\,$s, $T \sim 10^{27}\,\mathrm{K} \simeq 10^{14}\,\mathrm{GeV}$, when the Electroweak and Strong forces separate (see Lecture 7.1.3). Quantum fluctuations during the inflationary era grew to the temperature fluctuations at the level of $\delta T/T \simeq 1 \times 10^{-5}$ we see in the CMB photons emitted 372 000 years later from the surface of last scattering.

After photon decoupling, the photon-baryon fluid became a pair of gases, one of photons and the other of neutral hydrogen. Although the two gases coexisted spatially, they were no longer coupled together. The baryons, no longer tied to the photons, are from this point on free to collapse gravitationally, under their own gravity and that supplied by the dark matter.

Over the following 13.8 Gyr, gravity turned the tiny temperature fluctuations present at $z_{\rm dec}$ into the large structure in the distribution of galaxies we see around us today. We will return to this topic in Lecture 14. In the next lecture we will consider in more detail the wealth of information that can be deduced from the analysis of the temperature anisotropy of the CMB.

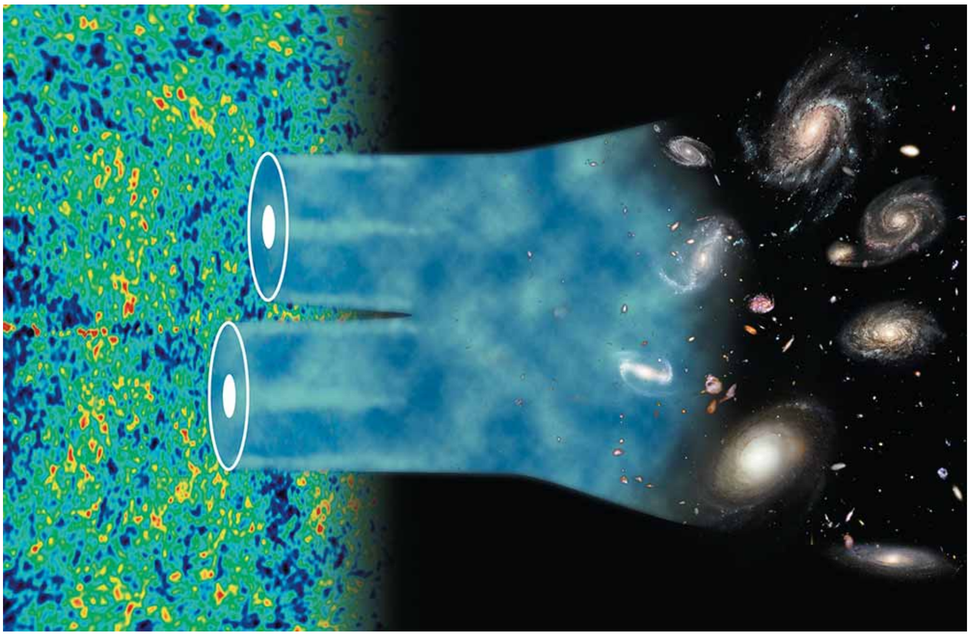

Figure 9.8: The large scale distribution of galaxies in today's (t = 13.8 Gyr) Universe can be traced back to the tiny temperature fluctuations present in the surface of last scattering at $t = 372\,000$ yr. (Figure credit: Chris Blake).